

# PIR Sensor Characterization and a Novel Localization Technique using PIRs

Sujay Narayana  
R. Venkatesha Prasad  
Vijay S. Rao  
Embedded Software Group  
Delft University of Technology  
The Netherlands  
SujayNarayana@student.tudelft.nl  
{rvprasad, vijaysrao}@acm.org

T. V. Prabhakar  
Sripad S. Kowshik  
Madhuri Sheethala Iyer  
Dept. of Electronic Systems Engineering  
Indian Institute of Science  
Bengaluru, India  
{tvprabs,sripadkowshik,madhuri}  
@dese.iisc.ernet.in

## ABSTRACT

Pyroelectric Infra-Red (PIR) sensors are used in many applications including security. PIRs detect the presence of humans and animals from the radiation of their body heat. This could be used to trigger events, e.g., opening doors, recording video, etc. PIRs are used widely because of their low power consumption.

Hitherto, PIR sensors were used for binary event generation – human/animal present or not-present. At the same time simple binary output hinders the use of PIR sensors in a wide variety of sophisticated applications. In the literature, we find limited characterization of analog output from PIR sensors that could provide much more information.

We built a simple array of PIR sensors and packaged them in a tower. We used two sets of four PIR sensors and tapped their analog signals after amplification. Our major contribution is the characterization of analog signals from the PIR sensors. We describe many interesting aspects obtained from the analog signals, which have not been explored until now. We also show their correspondence with the range, speed and size of the moving object. Using the characterization of PIR sensors analog data as well as simple binary decisions from these PIR sensors, we: (i) classify moving object with high precision; and (ii) localize the moving object. The major incentives are low operating power compared to WSNs.

We achieve 30 cm accuracy in 80% of the times, when ranging up to 5 m. Over multiple experiments for different persons in the range 1-10 m, we show that the error probability for localization is 0.08 at moderate distances (around 5-6 m). Our work will help in designing better detection and application triggers using PIR sensors in the near future. We believe that this work will open up new avenues in the development of new applications with PIR sensors.

Permission to make digital or hard copies of all or part of this work for personal or classroom use is granted without fee provided that copies are not made or distributed for profit or commercial advantage and that copies bear this notice and the full citation on the first page. To copy otherwise, to republish, to post on servers or to redistribute to lists, requires prior specific permission and/or a fee.

IPSN '15, April 14 - 16, 2015, Seattle, WA, USA

Copyright is held by the owner/author(s). Publication rights licensed to ACM.

978-1-4503-3475-4/15/04

<http://dx.doi.org/10.1145/2737095.2740886>

## Categories and Subject Descriptors

C.3 [Special-Purpose and Application-Based Systems]: Real-time and embedded systems; C.5.m [Computer System Implementation]: Miscellaneous

## Keywords

Pyroelectric Infrared sensors, PIR, ranging, localization, classification, detection, characterization

## 1. INTRODUCTION

Pyroelectric material based passive infrared (PIR) sensors detect any heat emitting body<sup>1</sup> moving in front of them. This ‘on the fly’ presence detection has found several applications, due to its inherent heat detection and measurement capabilities. For example, faucets open when hands are placed below; lights switch on/off when motion is detected in rooms; cameras are triggered on detecting movement of animals in their natural habitat for recording video. In the last example, a video sensor requiring higher power can be used efficiently with PIR sensors. Here a sensor that can “see” gets augmented with a sense of “feel” and this augmentation saves energy. Another major class of application is indoor security systems.

PIR sensors can be made to do more: range and localize objects for use in security systems and gaming applications. In these applications, if only camera sensors are used, they consume more power for sensing a large area; they require sophisticated image processing algorithms and expensive lenses to improve ranging and angle of detection. For example, Microsoft Kinect [3] uses a camera with sophisticated algorithms for ranging to drive gaming applications. Wireless Sensor Networks for localization require beacons and exchange of information packets in range-based algorithms [11] and dense deployment in range-free localization [14]. Thus the ultra low power feature of PIR sensors becomes attractive. Typically, a PIR sensor consumes approximately  $3 \mu\text{W}$  for movement detection and corresponding amplifiers consume  $800 \mu\text{W}$ . Further, by employing PIR sensors that cover disjoint but adjacent areas along with simple-to-mount plastic lenses (to improve the range of sensors), we can reduce

<sup>1</sup>In this article, we refer to the heat emitting sources as objects that consist of warm-blooded living beings including humans and other sources.

the power consumption by several orders. Thus, PIR sensors provide a low cost, low power, inexpensive, small and lightweight alternative in many applications, if exploited in the right way.

Unfortunately, many of the existing works are interested in the binary output. Typically, applications (for example, robot tracking [10]) that uses binary output from the PIR sensors. The right way, we believe, is to utilize the analog output from the PIR sensors. In fact, we can exploit information provided by amplitude, phase and frequency of the analog signal from PIR sensors for detection, ranging of the object, etc. For instance, the analog signal can not only detect the presence of a human, but also his/her height, direction of movement, how far he/she is from sensor system. If the person has a special gait or gesture associated with his walk, the signal could have rich information to identify or at least differentiate people, which is not possible with binary output. Since characteristics of the analog signals from PIR sensors are not well-studied, there is a gap in literature. To this end, we first characterize the analog output.

With the analog signals, we specifically target two important problems: (i) Detection and classification: finding the moving object fairly accurately, and classifying the object's width and height. (ii) Localization: the so-called "Holy Grail" application of sensor networks – *the localization of objects*<sup>2</sup>. In the process, we go beyond the conventional use of PIR sensors and show that we can extract several new features from PIR sensors.

A known problem of PIR sensors is that they are very sensitive to slight disturbances – even fluttering of leaves or a blowing of hot air during the summer months can trigger a presence, leading to false alarm or low detection rates. Many techniques and sophisticated machine-learning algorithms have been developed to improve true detection. In order to avoid this problem, we have used multiple collocated PIR sensor arrays in order to detect and classify objects with reasonable certainty.

We have modified the PIR reference electronic design to get analog signals for processing. Our contributions are of several folds: (a) we have provided an in-depth discussion of the important characteristics of the analog signal from the PIR sensors that may be used in applications other than ones discussed in this article; (b) our system containing an array of PIR sensors can be used for different applications such as moving object classification and localization; (c) we have classified the height and width of the detected object; (d) we have proposed novel methods of using the analog signal for continuous ranging and localization. To the best of our knowledge, this work is one of the first to exploit analog signals. We believe our work can open up new avenues for research using PIR sensors, possibly in many different ways.

The rest of the article is structured as follows: In Section 2, we describe some of the previous work on PIRs that are close to ours; in Section 3 we describe our experimental setup; in Section 4 we characterize analog output signals from PIRs. We explain classification in Section 5, and localization in Section 6. We describe the evaluation of our system in Section 7, and finally conclude in Section 8.

## 2. RELATED WORK

In literature, many applications use multiple PIR sensors

---

<sup>2</sup>We consider only indoor environments for localization.

either as an array of collocated sensors or distributed in space mostly using binary output. Complex techniques and algorithms are then employed to achieve applications such as localization. We list some of the relevant applications and how they are executed.

*Counting:* Wahl et al. proposed a distributed PIR sensor based algorithm for detecting and counting people [13]. Binary output from PIR sensors is used to reduce the overhead of continuous sampling and in turn reduce the energy consumption.

*Detection:* Analog signals rendered by the PIR sensors are analyzed to distinguish true intrusion from clutter due to vegetation has been studied by Abu Sajana et al. [4]. Encouraged by the results, authors in [4] extended it for intrusion classification using chirplets [12]. We collaborated with them to develop a PIR sensor platform as described in this paper. Moving beyond the use of binary output for motion detection, Frankiewicz and Upik explore the hardware requirements to extract analog signals for motion recognition and activity classification [8]. Al-Naimi, et al. used a combination of custom built PIR sensor and embedded pressure sensors to accurately detect, identify and track humans [6].

*Tracking:* Xiaohu and Yongxin used a crawler robot with modified pyroelectric sensor mounted on it to track humans and animals and also determine the direction of motion [5]. Jaeseok and Min-Hwan designed a ceiling mounted array of sensors to detect the direction of motion utilizing dual element sensors arranged in  $2 \times 2$  matrix and polarized analog output [15]. Tracking people moving in a hallway using the similar principle is reported in [18]. PIR sensors facing each other throughout the hallway are used to localize people.

*Localization:* Zhiqiang et al. used PIR sensor in both indoor and outdoor settings to detect and localize moving targets [19], where a grid network is used assisted by an adaptive thresholding to find direction. Localization of humans in an indoor environment using an array of PIR sensors fixed on the ceiling is discussed in [9]. Signal from multiple PIR sensors are mapped onto a feature space using temporal and spatial correlation. Location is estimated using intersection probability. We also show some important differences between GridEye [2] sensors for localization with ours in Table 1. Feng et al., harnessed IR changes induced by human motion using PIR sensors and show its advantage over acoustic, ultrasonic and optical sensors for detection and localization applications [7]. Localization is done using the binary output coming from three IR bearing arrays each consisting of four vertically mounted PIR sensors. Position identification of a human using a pair of PIR sensors is reported in [17]. The sensors are placed facing each other and the area between them is separated into three zones. Depending on the number of sensors triggered, position in terms of zones is found. Some basic features, such as duration and output amplitude, are measured to further refine the position of the person. Zappi et al. proposed a system where three PIR sensor systems are placed at an angle with respect to each other [16]. They distinguish the direction of movement and count the number of people moving through a gate or a section of a hallway. A portion of the Fresnel multi-lens is masked to create a narrow slit and achieve the required Field of View (FoV) to suit the application requirements.

As described above, most of the proposals use binary output to achieve their goals. While analog signals are used by

some [16, 17], they at most use them in a rudimentary fashion. None of these works have harnessed analog signals for ranging and localization of people moving randomly. This may be because analog signals have not been characterized thoroughly. Of these works, though Zappi’s work is not for ranging it uses multiple sensors to gather analog signals [16]. This seems to be the closest work to that of ours. We also compare our work with [16].

Table 1: Comparison with GridEye [2] and Melexis [1]

| Parameters               | Our Work   | GridEye  | Melexis  |
|--------------------------|--|--|--|
| Sensing Element          | Pyroelectric   | Thermopile                                     | Thermopile                                     |
| Sensing Property         | Senses Temperature Difference seen by two sensor elements      | Direct indication of the incident IR flux      | Direct indication of the incident IR flux      |
| Sensing Range            | 15-20m (adjustable)  | 5m   | <10cm  |
| Power                    | 6.75mW   | 22.5mW   | 6mW  |
| Signal Type              | Analog   | Digital  | Digital  |
| Detection                | Only moving objects  | Both static & moving objects                   | Both static & moving objects                   |
| Range Estimation         | Yes  | No   | No   |
| Complexity               | Low (only post processing required)                            | High (embedded DSP & post processing required) | High (embedded DSP & post processing required) |
| FoV                      | 16.73° (conical) Spot, 97° horizontal & 4° vertical Multi-lens | 60° conical                                    | 90° conical                                    |
| Sensing elements/ pixels | 16   | 64   | N/A  |

### 3. EXPERIMENTAL SETUP

Since we are interested in capturing analog signals from PIR sensors, we have designed a custom-made system for our experiments. We detail our setup in this section.

#### 3.1 Sensor Tower Design

A single PIR sensor cannot provide much information about a moving object in order to classify and localize it with reasonable accuracy. To achieve this, we collaborated with [12] and designed a sensor tower with collocated multiple PIR sensors in a specific configuration. We have also built an appropriate electronic circuit to capture the analog signals for processing rather than working with binary output as provided in the vendor reference circuits. Figure 1 shows the PIR sensor tower, which houses collocated multiple PIR sensor arrays covered with lenses that support different angles and ranges for detection. The tower is bifurcated into “Group A” and “Group B”, each consisting of a pair of quad-element sensors where each sensor provides two analog outputs. Each quad-element sensor is mounted in such a way that the two dual-element sensors inside are vertically one above the other. Group A has two spot lenses, covering dual-element sensors, namely S1 and S2, and S3 and S4. Group B also has two dual-element sensors, namely M1 and M2, and M3 and M4, that are behind multiple Fresnel lenses (called multi-lens hereafter). Further, we can change the gain of Group B sensors thereby we can adjust the detection range, which helps in localization.

Typically, detection area of a PIR sensor element is small and rectangular in shape. In order to sweep a larger area and to strengthen the incoming infrared rays, we have placed Fresnel lenses in front of the sensors. Such a lens condenses the incoming infrared rays into its focal point where the sensor is mounted. We use different types of lenses that

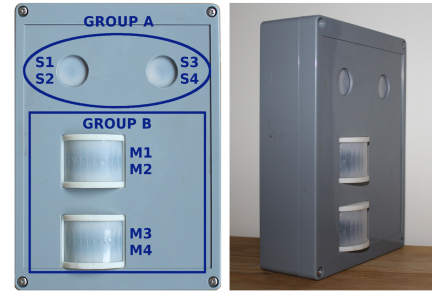


Figure 1: PIR sensor tower system.

cover Group A and Group B sensors, since their purposes are different.

The spot lens used are TR1004 from Kube<sup>3</sup>. The purpose of the spot lens is to get a narrow angle of detection so as to find the width of the moving object. The spot lens has a conical angle of 16.73°. The multi-lenses used are TR426 also from Kube. The intention of placing these multi-lenses is to cover wider angle and provide better range of detection. The multi-lens has 97° along the horizontal plane and 4° angle along the vertical plane. A multi-lens is made up of 10 small “lenslets”. An object moving in front of these sensors cuts the beams of detection rendering an output that holds information about the object. The multi-lens sensor in the top is shifted 2.2 mm downwards from the focal point so that the FoV points upwards. Similarly, the bottom multi-lens sensor is shifted upwards from the focal point by 2.2 mm to bend the FoV downwards. This mechanism avoids the overlapping of FoV of both multi-lens sensors, providing a larger range for height classification.

Due to this configuration of sensors and lenses, the tower provides us details on height and size of the detected object, and paves a way for better classification and localization algorithms.

#### 3.2 Electronics

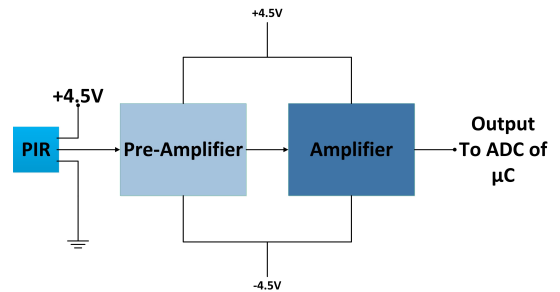


Figure 2: PIR amplifier circuit.

The signals from PIR elements are weak and need to be amplified several hundred times to get a reasonable signal to work with. Further, a single rail amplifier design reference provided by the vendor can result in a smaller swing of the analog signal. Hence, to gather the true analog signals, we drive the op-amp with a “Rail-splitter” system. The rail-splitter takes the conventional single rail from a 9V DC supply and splits it to dual rail for use by amplifiers. The

<sup>3</sup><http://www.kube.ch>

electronics shown in Figure 2 consists of a two-stage amplifier. The gain of each stage is adjustable using a potentiometer placed at the feedback of each stage. Therefore a dual sensor PIR has four potentiometers with which we can adjust the gain. We explain the capabilities of this circuit that provides more opportunity to extract features from analog signals where signal amplitude, phase and frequency with parameters such as amplifier gain assist in analyzing the signal for detection and ranging.

## 4. CHARACTERIZATION OF SIGNALS FROM THE SENSOR TOWER

We first look at the analog signals obtained from the sensors, before describing the features of the signals.

### 4.1 Analog Output of the PIR Sensors

The principle of operation of the sensors is as follows: dual-elements of a single sensor (e.g., S1) are wired as opposite inputs to a differential amplifier. Thus, output from one element has its polarization inverted compared to the other. When an object passes by, the sensor gets triggered by one of the elements, producing a differential voltage between two elements of the sensor. This corresponds to the ‘positive’ output, i.e., a positive voltage is generated. When the object crosses the other element, the polarization reverses resulting in ‘negative’ output. When an object moves across the sensor tower (parallel to the face of the tower) in the FoV from one end to the other, the analog signals generated by a spot sensor and a multi-lens sensor are shown in Figure 3. Since the sensors at the top of the tower are covered with spot Fresnel lenses, ‘positive to negative’ and ‘negative to positive’ swings are generated. However, since multi-lens have 10 lenslets, they generate a sinusoidal swing as the object moves across. Here, each sinusoidal swing corresponds to one lenslet of the multi-lens, indicating detection of the object.

To the best of our knowledge, we are the first to sample PIR analog signals at 1 kHz. The raw signals obtained from all the sensors are smoothed using Savitzky-Golay filter. This helps in removing the minor peaks caused by noise. Thus peak to peak amplitude can be found effectively.

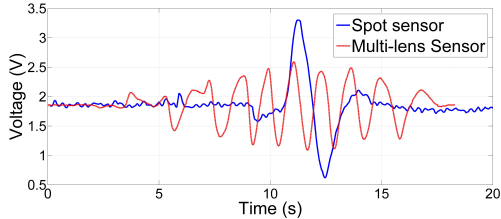


Figure 3: Output signals generated by spot and a multi-lens sensor on detection.

### 4.2 Characterization

PIR sensors are very sensitive to any change in the incoming IR rays; even the smallest movements are registered. To increase reliability, we combine analog signals from multiple sensors in the system. This increases the accuracy of identification and even estimation of the behavior of movement as compared to what a single PIR sensor can achieve. To demonstrate this, we conducted a simple experiment in

| System          | False alarm (%) |
|-----------------|-----------------|
| One PIR Sensor  | 17.5            |
| Proposed system | 2.5             |

Table 2: Comparison of false alarm rate in proposed system to a system using only one PIR sensor.

which an object moves randomly across our sensor tower and a PIR sensor. Table 2 shows that our system can reliably detect objects due to combining the output of multiple sensors.

From the analog output signals of the sensor tower we observe several parameters – such as, frequency and amplitude – that depend on the characteristics of movement by the object. We collected the parameters by deploying the sensor tower and repeated the experiments to get consistent measurements. We describe the parameters below.

#### 4.2.1 Amplitude (A)

The amplitude of the output signal from each sensor indicates the difference in heat (of IR rays) detected by each sensor element. Each sensor unit (see Figure 1) continues to provide signal output until their dual-elements do not see a change in the temperature. We observed several factors that impact the amplitude of the signal.

Ambient temperature plays a crucial role in the detection of a moving object. The amplitude of the analog output from a PIR sensor is directly proportional to the difference in temperature of the object and the ambience. Figure 4 shows the peak to peak amplitude of the output from the spot sensor (whose gain is relatively high) at 1°C and 20°C of a person walking. This can affect the localization process when the amplifier gains are low. We have not compensated temperature in ranging. However with the help of an extra circuitry including a thermistor it is possible to compensate the error due to ambient temperature in the localization process.

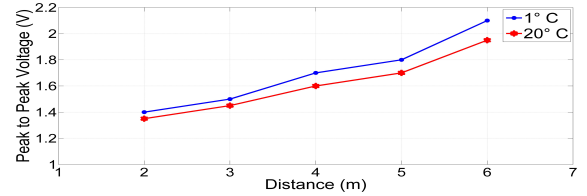


Figure 4: Effect of temperature on amplitude.

#### Gain of the amplifier (G)

The gain of the amplifier controls the sensitivity of the PIR sensors. By changing the sensitivity, it is possible to change the range in their FoV. Sensors can detect motion at longer distances – when the output signal is amplified with a higher gain – due to relatively higher amplitude of the output signal. Thus, the gain plays a crucial role in setting the range of detection ( $R$ ) in the FoV of the sensor.

#### Speed of moving object (S)

With a constant gain set for all the sensors, we observed that as the speed of the moving object at a particular distance increases, the amplitude of the output signal decreases. This is because the duration and amount of IR rays falling on

the sensor element diminishes as the speed of the moving object increases. When the object moves slowly across a sensor, the exposure time of the object is longer. Longer the duration, higher is the chance of absorbing all the IR rays emitted by the object, and thus, generating relatively higher amplitude. Figure 5 plots the variation in amplitude of the output signals generated by a spot sensor and a multi-lens sensor at three different speeds 1kmph, 5kmph and 10kmph. The distance of the object from the tower is kept constant in all the experiments.

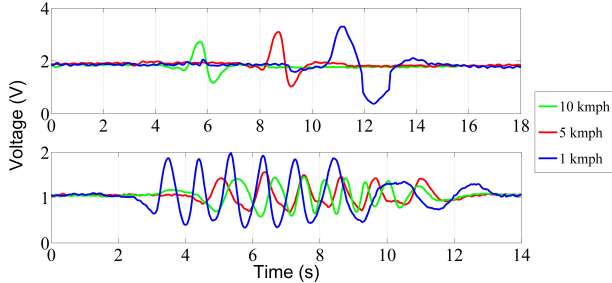


Figure 5: Plots showing the output signals from a spot sensor (top) and a multi-lens sensor (bottom) at different speeds while keeping the gain and distance constant.

### Distance of moving object ( $D$ )

Peak-to-peak amplitude is an important feature that was not harnessed hitherto. For a particular gain, with fixed speed of movement, we measured the peak-to-peak amplitude of the output signal from a multi-lens sensor and a spot sensor. We varied the distance of the moving object from the tower, and the object moved across while facing the tower. We collected these measurements asking 20 people to move across the tower with a timer. Each data point is the average of 20 experiments. The peak-to-peak amplitude for various distances forms a bell-shaped curve as shown in Figure 6. Interestingly, we see in the plot that the peak-to-peak amplitude increases with the distance initially, but gradually decreases and, finally, vanishes. The reason for this behavior is almost similar to that of the speed of movement. When a person moves across the sensor in the proximity, he is nearer to the vertex of conical FoV of the sensor element. In this case, the duration for which he is in the FoV of the sensor is relatively low compared to that of movement farther away. Hence, the amplitude of the signal is low for movements nearer to the tower. Similarly, at farther distances, because of diffusion of the IR rays in the ambiance, IR rays absorbed by the sensor elements are not sufficient to generate high amplitude. Consequently, there is an optimal point between the nearest and farthest distance, where the amplitude of the signal is highest. Around this distance, the sensor receives maximum amount of IR radiations from the moving body to generate high amplitudes. Note that the speed and gain influence this amplitude. The amplifiers of spot and multi-lens sensors having the same gain, the peak-to-peak amplitude generated by spot sensor was observed to be relatively higher compared to that of multi-lens. This is because, the spot lens had larger aperture than that of each lenslet in the multi-lens. Hence, spot sensors can target larger ranges.

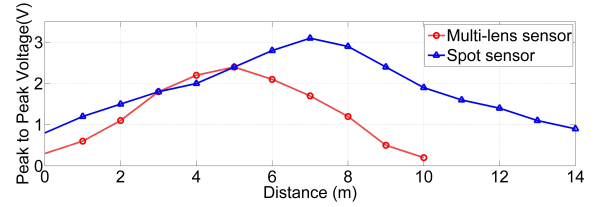


Figure 6: Example plots showing the peak-to-peak amplitude of output signals from a spot sensor and a multi-lens sensor for movements at different distances with same gains and speed set to 4 kmph.

### Orientation of motion ( $\theta$ )

The amplitude of the signal varies as the orientation of the object changes while keeping the speed constant. When the object moves towards the sensor at a distance at an angle  $\theta$  with respect to the face of the tower (for instance,  $45^\circ$ ), the peak-to-peak amplitude generated by a lenslet of the multi-lens is comparatively more with respect to the output from the immediate previous lenslet. Similarly, when the person moves away from the sensor tower at an angle  $\theta$  to the face of the tower, the amplitude decreases gradually with time. However, this phenomenon cannot be observed in spot sensors as each element generates only one swing on detection. The decreasing peak-to-peak amplitude when a person moves towards the tower crossing the FoV of sensors at the angle  $45^\circ$  is shown in Figure 7. The angle of scope ( $\phi$ ), shown in the figure varies as the orientation of motion changes.  $\phi$  is maximum when the movement is perpendicular to the sensor face. However,  $\phi$  depends on the speed of movement. At a speed of 1 kmph, and a  $\theta$  of  $45^\circ$ ,  $\phi = 140^\circ$  and for 10 kmph,  $\phi = 170^\circ$ . When the movement is parallel to the sensor tower at any constant speed over time  $\phi = 90^\circ$ . Once we know the speed (see Section 6.2.2), we can calculate the angle  $\theta$ . As an illustration, we found the following relationship between  $\theta$  and  $\phi$  empirically for an object moving at 5 kmph:  $\theta = 0.8867\phi + 91.3$ .

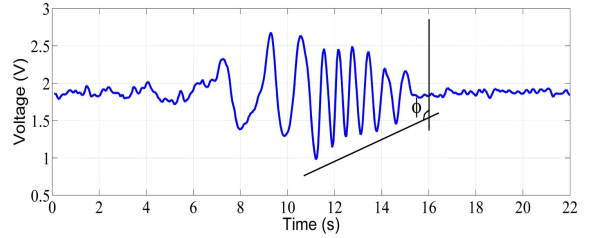


Figure 7: The variation of amplitude and frequency for the movement at an angle  $45^\circ$  at a speed of 5 kmph.

#### 4.2.2 Frequency of the observed signal

Because of multiple lenslets in the multi-lens sensors, the output signals from these sensors contain sinusoidal waves whose frequency changes with the change in distance and/or speed of movement. When the object moves at a constant speed at nearby distances across the tower, frequency of the signal is higher as the object cuts more lenslets in lesser time. At farther distances, the conical FoV grows and the object will take more time to cross single lenslet at the given speed. When the distance is kept constant, frequency of the

signal is directly proportional to the speed of movement. Figure 7 shows the increase in the frequency of signal, when the movement is towards the tower from a farther point, at an orientation of  $45^\circ$ .

#### 4.2.3 Phase of the signal

The phase of the output signal generated by the spot sensors indicates the direction of movement. When the movement is from left to right, the left sensor element of a dual-element sensor (say S1) is triggered first. This generates a positive pulse. When the object crosses the right sensor element, then a negative pulse is generated. The output waveform is shown in Figure 8. Similarly, if the direction of movement is from right to left, the sensor element in the right triggered first which generates a negative pulse, succeeded by a positive pulse by left element. Hence, the direction of movement can be identified observing the behavior of the spot sensors.

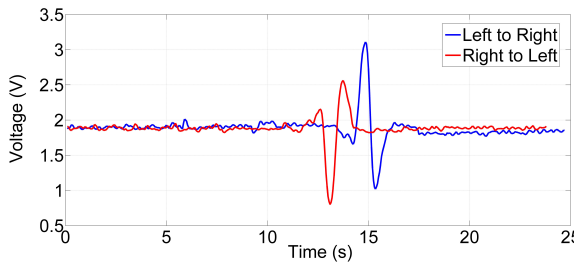


Figure 8: Plot showing the phase of output signal from a spot sensor for a direction left to right and right to left.

#### 4.2.4 Time difference between pulses of spot sensors

Unlike the multi-lens sensors, the spot sensors at the top of the tower will generate a single pulse when the object is detected. When the moving object enters the FoV of one of the spot sensors (for instance, S1), the sensor generates a sinusoidal swing. When the object leaves the FoV and enters the FoV of another spot sensor (for instance, S3), there is another pulse generated by the second sensor. Hence, the time difference between the pulses generated by sensors on the left and right of the tower is the time taken by the object to move from the outer end of FoV of the left sensor to the extreme end of the FoV of the sensor on the right. The period of the pulse generated by a sensor is equal to the time taken by the object to cross the FoV of the corresponding sensor. Figure 9 shows the time at which the object is in front of spot lens S1 (blue pulse) and the time at which the object enters the FoV of S3 (red pulse). Considering the object is moving across the sensor tower, as marked in Figure 9,  $t_1$  is the time taken by the object to move into the FoV of S1 and exit S3,  $t_2$  is the time the object being in the FoV of S1; and  $t_3$  is the time in which the object is in the FoV of S3. Thus, spot sensors give the information about the angle of moving object in the FoV at a particular time instance.

## 5. CLASSIFICATION OF OBJECTS

It is possible to estimate and classify the height of objects being tall or short. Similarly, the width of the object can also be classified into small or big. This may be important information in indoor security systems. For example, with

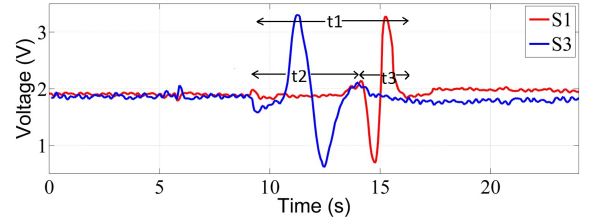


Figure 9: Plot showing the time differences between two detections.

the height and width information, one may draw inference on the type of object: a tall and small object could be a person, and a short and big object could be a pet. This information can avoid false alarms caused by pets when the sensors are deployed indoors for security purposes. We make use of spot sensors and multi-lens sensors together to classify the height and width of moving objects. For classification, all the sensors are set with a fixed amplifier gain so that the detection range in the FoV can be set. Each sensor output is considered to examine whether there was detection or not in the FoV of that particular sensor.

## 5.1 Height classification

We use the multi-lens sensors to estimate the height of moving objects. If the detection is triggered by all the four multi-lens sensors M1, M2, M3 and M4, then we classify the object as “Very Tall”. On the contrary, if there is detection by M4 alone, then the height of the moving object is classified as “Very short”. In this way, depending on the detection by different sensors, we can easily classify the height of the detected object into four categories – “Very short” (detection by M4 only), “Short” (detection by M3 and M4), “Tall” (detection by M2, M3 and M4) and “Very Tall” (detection by all multi-lens sensors). Figure 10 shows an example of height classification of an animal. Since the object is detected by M3 and M4, we can say that the height falls in the “Short” range. The decision, of course, depends on the distance; thus ranging before classification is necessary for higher accuracy.

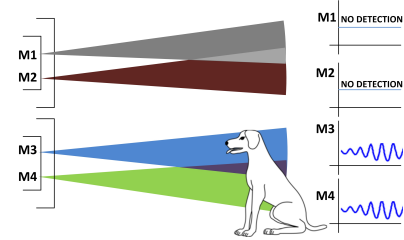


Figure 10: Side view of an animal in the FoV of M3 and M4.

## 5.2 Width classification

We use the spot sensors for width classification. When a person moves in front of the sensor tower, it is possible that spot sensors (either S1 and/or S2, or S3 and/or S4) can trigger at an instant. However, in case of big animals (like cattle in outdoor settings), all the spot sensors trigger at the same time when animals are in the FoV of all the spot sensors. Even pets like dogs can trigger two sensors at the same time. Hence, we classify the object that is detected

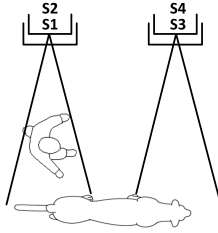


Figure 11: Top view of a walking person and an animal in the FoV of spot lenses.

by the sensor(s) (S1 and S2 or S3 and S4) at an instance as “Small” and detection by at least one on both sides as “Big” (see Figure 11).

Though spot sensors are majorly responsible for width classification, multi-lens sensors can also help in this case as they generate sinusoidal waves when the object moves across them. For a particular speed of movement, the frequency of the signal generated by multi-lens sensors is more when a four-legged animal walks in front of it compared to a human. Four legs cut different lenslets of the multi-lens at a faster rate one after the other unlike in the case of a human. Though we classify objects in terms of big, small, tall, etc., it is also possible to estimate the height of the object to a certain extent. This can be achieved once the localization is done. The height at which the sensor tower is placed is known. When the distance of the object from the tower is estimated, the height of the object can be calculated using the geometry of the FoV of the sensors, which is a constant parameter. For instance, if the tower is placed at a height of 1 m from the ground, then the outer edge of the FoV of M1 covers a height of around 2.5 m at a distance of 8 m from the sensor tower. Hence, we can specify very short, short, tall and very tall as less than 1 m, between 1 and 1.5 m, between 1.5 and 2 m and greater than 2 m, respectively.

## 6. LOCALIZATION USING SENSOR TOWER

In this section, we first describe different techniques for ranging. Then we describe our novel ranging and localization techniques.

### 6.1 Localization with fixed gain

We localize an object by considering the parameters (see Section 4.2) from all the signals that capture the movement. We have tried to localize objects using different approaches. In order to achieve localization, it is necessary to find the range of the moving object from the tower, its direction, speed of movement, and the angle at which the object is moving with respect to the sensor tower.

#### 6.1.1 Fixed gain

Through controlled experiments we first try to find the exact relationship between the signal parameters such as amplitude and frequency for movements at various speeds at different distances and angles. In this experiment, all the eight sensors had a constant gain, which was tuned for the sensor sensitivity to cover a range of approximately 7 m from the sensor tower in the FoV. The experiment was conducted in an indoor area (classroom). The sensor tower was placed in one end of the room at a height of around 1 m from the ground. The tower was placed in such a way that the maximum area of the room is covered by the FoV of the sensors.

Several trials were done by moving at different speeds and at various distances with a step of 1 m until the end of FoV, i.e., at 7 m. We repeated this experiment with and without obstacles such as desks and benches in order to find the effect of obstacles on the sensor output.

After processing the output signals, we were able to find the speed and distance of the object manually for each particular trial. The obstacles did not affect the output signal noticeably unless the obstacle covered the object completely. With the measurements and characterization, it is not possible to derive a relation between the signal parameters as all of them are interdependent on each other except the amplifier gain. In addition, signals generated by the sensors could be the same if an object moved at a higher speed at farther distance or if the object moved at a lower speed at a nearer distance. Hence, at least one of the signal parameters or a physical parameter has to be found in order to estimate the other.

#### 6.1.2 Trilateration using multiple towers

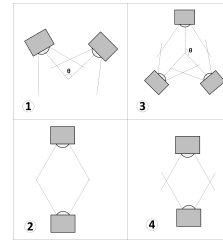


Figure 12: Multiple towers deployed.

As a next step, we used more than one sensor tower for localization so that trilateration could be applied. When more than one tower was used, each tower looked at the moving object from a different angle and a different distance. With the combination of signals from different towers placed at pre-defined locations, it was possible to overcome the parameter dependency problem and arrive at an acceptable conclusion. A few possibilities for placing the sensor towers are shown in Figure 12. The combinations include the placement of two sensor towers along a horizontal line (Fig. 12-1) or vertically opposite to each other with FoV of two towers not overlapping (Fig. 12-2), three sensor towers along a circle at an angle of 120° with respect to each other (Fig. 12-3) and vertically opposite with non-overlapping FoV (Fig. 12-4). The experiment was conducted in the same location as earlier, but with two sensor towers that were placed 5 m apart. The towers were kept at an angle of 70° with respect to each other to get maximum overlapping FoV. The experimental results showed the possibilities of localization with multiple towers but the signal processing was more complex due to many outputs. Another disadvantage of this method was that the towers had to be kept at specific angles during deployment. A small change in the placement might lead to inaccurate estimations.

#### 6.1.3 Energy output over time

The elements of a PIR sensor are of a capacitive nature. The energy of the signal output from the PIR sensor is directly proportional to the amount of heat absorbed by the sensor elements and is accumulated at the elements acting

as a capacitor. Hence, the output current is inversely proportional to the output voltage of the signal. Hence, energy  $E$  of the signal from sensor is,  $E = I \int_{t_1}^{t_2} y(t) dt$ , where  $I$  is the current output and  $y(t)$  is the time variant analog signal from the sensor. The integration of the output from multi-lens sensors over time is the energy output by the sensor, which depends on the amplitude and frequency of the signal. Here a question arises: what if the energy output from a sensor is the same for different speeds of movements at different distances? Even though the signal parameters are interdependent, this problem can be tackled easily as the combination of amplitude and signal frequency is unique in different scenarios. Certainly, the output energy of the signal is equal for a slower movement at nearby distances and for a faster movement at farther distances. But peak-to-peak amplitude is inversely proportional to the frequency in this case, providing a unique solution.

## 6.2 Localization with variable gain

All the experiments done until this stage were with fixed gain. Modifying the amplifier gain results in a change of the sensor sensitivity, implying change in the detection range. Thus, by setting different gains for different amplifiers, it is possible to create specific ‘zones’ of distances until which a particular sensor detects the motion. Now, we have two parameters: gain and the range, whose values are fixed. We conducted an experiment using a single sensor tower with different gains set for spot and multi-lens sensors with which we could achieve localization successfully.

### 6.2.1 Zoning or Ranging

Several zones in the FoV were created by adjusting the amplifier gain for the multi-lens sensors. Here, only the multi-lens sensors were used for zoning as they have a wider FoV and also because of their ability to generate continuous sinusoidal signals when compared to spot sensors.

#### Gain adjustments

We refer to a multi-lens sensor in the tower as  $M_x$  where  $x \in \{1, 2, 3, 4\}$ . Each multi-lens sensor  $M_x$  was set with an amplifier gain  $G_x$  so that the output signal with maximum peak-to-peak amplitude  $A_x^{max}$  occurs only at a particular distance  $d_x$  at a reference speed  $S_{min}$ . This reference speed was usually very low because the sensor generates maximum voltage at relatively low speeds of movement only if the heat emitted by the object moving across the tower is captured well. Thus, the gain for the amplifiers was set according to the speed  $S_{min}$ . All the spot sensors had the same gain set to cover a maximum detection range of  $2d_{max}$ , where  $d_{max} = \max\{d_x\} \forall x$ .

#### Zone creation

The value  $d_x$  for a particular sensor  $M_x$  had to be chosen wisely so that new blind areas were not created in the FoV. Hence, one dual-element sensor of a quad-element sensor had to cover the maximum possible range. So, it is wise to set sensor M1 to generate maximum peak-to-peak voltage output at  $d_2$ , M3 at  $d_4$ , M2 at  $d_3$  and M4 at  $d_1$ , where  $d_4 > d_3 > d_2 > d_1$ . The inter-zonal distances, which is the distance between  $d_2$  and  $d_3$  or between  $d_3$  and  $d_1$ , and so on, can be arbitrarily set. However, the localization is more accurate only when these values are equal and as small as possible. A typical inter-zonal distance is around 1 m

which is sufficient enough to locate a moving person in a small room. If the value is below 1 m, then the fine details of hand movements might be recorded creating ambiguity during signal processing. This inter-zonal distance decides the resolution of the localization. The ray diagram with FoV of each sensor after setting variable gains is shown in Figure 13. The output of sensor M1 is  $A_{1,max}$  at distance  $d_2$ , output of M2 is  $A_{2,max}$  at distance  $d_3$ , output of M3 is  $A_{3,max}$  at distance  $d_4$  and output of M4 is  $A_{4,max}$  at distance  $d_1$ . The  $d_1, d_2, d_3$  and  $d_4$  are set as 1 m, 2 m, 3 m and 4 m, respectively.

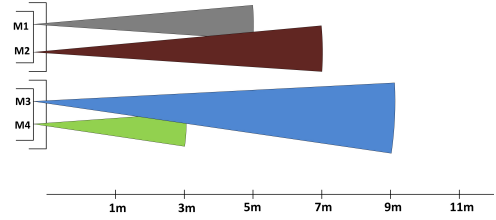


Figure 13: Ray diagram after setting variable zones.

#### Amplitude vs Distances/zones

As explained earlier, the plot of peak-to-peak amplitude  $A_x$  v/s distance  $d_x$  forms a ‘bell’-shaped curve whose peaks are at the same distances. This is true when the amplifier gain of the multi-lens sensors are the same. In case of different gains set for different multi-lens sensors, the peak of each bell shaped curve shifts by  $d_x$  where the corresponding sensor  $M_x$  generates maximum peak-to-peak voltage  $A_x^{max}$  as shown in the top plot of Figure 14. Because of different zonal coverage,  $A_3 > A_2 > A_1 > A_4$  at particular distance  $d_x$ . In general, the output signal from the sensor  $M_x$  has maximum peak-to-peak voltage  $A_x^{max}$  at distance  $d_x$  when an object moves across the sensor at speed  $S_{min}$ . At distances shorter and longer than  $d_x$ , the amplitude of the signal  $A_x$  from the sensor  $M_x$  decreases gradually until it reaches almost zero. However, for the movement at farther distances, the object is out of range, thus, the signal is almost zero. At nearby distances, say less than 1 m from the tower, the object is almost in the vertex of conical FoV of a sensor and, thus, both the elements of the sensor see the same temperature resulting in near zero output.

### 6.2.2 Speed Calibration

The reference plot (top) in Figure 14 is obtained for speed  $S_{min}$ . In real-time, the object can move at different speeds at different instances. Hence, it is necessary to consider the variation in peak-to-peak amplitude of the output signal at different distances for different speeds. The plots of maximum peak-to-peak amplitude  $A_x$  vs distance  $d_x$  for sensors  $M_x$  for speeds  $S_i$ <sup>4</sup> and  $S_{max}$  is shown in Figure 14 (middle and bottom plots, respectively). Since the reference plot is obtained for the lowest considered speed  $S_{min}$ , the speeds  $S_i$  and  $S_{max}$  are higher than  $S_{min}$  i.e.,  $S_{min} < S_i < S_{max}$ . Although in experiments we tested for various speeds, we plotted three curves of reference speeds in Figure 14 for brevity. If a set of curves for a particular speed is available then we use the measurements. Otherwise, we use interpolation. At

<sup>4</sup> $S_i$  is the speed of object which is between  $S_{min}$  and  $S_{max}$ .

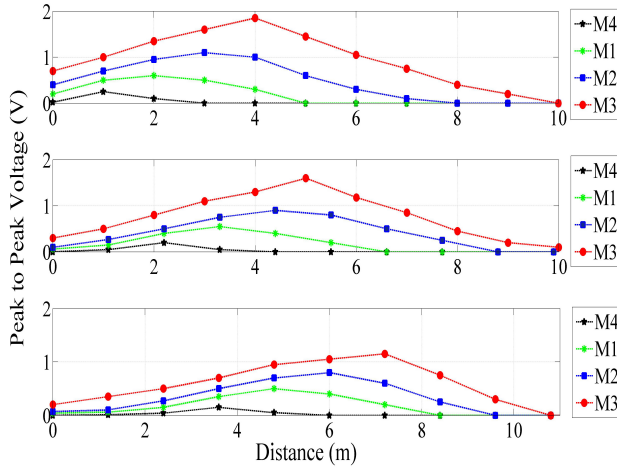


Figure 14: Peak-to-peak amplitude vs distance at speeds  $S_{min} = 1$  kmph (top),  $S_i = 5$  kmph (middle) and  $S_{max} = 10$  kmph (bottom).

speeds  $S_i$  and  $S_{max}$ , the plot obtained is a set of bell-shaped curves, but the maximum peak-to-peak amplitude  $A_x^{max}$  for sensor  $Mx$  is less than  $A_x^{max}$  obtained with speed  $S_{min}$  for the same sensor. Moreover, the distance at which  $A_x^{max}$  occurs is not at  $d_x$  anymore, but at  $d_x + \delta$ , where  $\delta$  is a small increment in distance. This means, at speed  $S_i$ , the entire reference plot is shifted to  $d_1 + \delta_1$  along abscissa and shifted to  $d_2 + \delta_2$  for speed  $S_{max}$ . This phenomenon is because of the dependency between speed, distance and amplitude as explained in Section 4.2. Correspondingly, the decrease in amplitude is also observed for higher speeds. These set of plots obtained with speed  $S_{min}$ ,  $S_i$  and  $S_{max}$  are used as reference on the fly to localize an object if the curves for different (intermediate) speeds are not available.

### 6.2.3 Signal Processing

The three set of curves obtained at speeds  $S_{min}$ ,  $S_i$  and  $S_{max}$  can be mathematically represented using Gaussian curve fitting. In order to increase the accuracy of the fit, two terms were considered. Now, each curve has the expression in the form,

$$A_{x,S}(d) = a_{1(S,d)} \exp\left(-\frac{(d - b_{1(S,d)})^2}{c_{1(S,d)}^2}\right) + a_{2(S,d)} \exp\left(-\frac{(d - b_{2(S,d)})^2}{c_{2(S,d)}^2}\right),$$

where  $x$  is the multi-lens sensor (M1, M2, M3 or M4),  $S$  is the reference speed ( $S_{min}$ ,  $S_i$  or  $S_{max}$ ) and  $d$  is the distance. Hence,  $A_{x,S}(d)$  gives the peak-to-peak amplitude of the output signal from multi-lens sensor  $x$  at distance  $d$  for the particular reference speed  $S_i$ . The coefficients  $a_1$ ,  $a_2$ ,  $b_1$ ,  $b_2$ ,  $c_1$  and  $c_2$  are the coefficients obtained from curve fitting, which are constant for the respective curves. Considering this Gaussian fit and the coefficients, the speed of movement and the distance of the moving object from the sensor tower can be estimated using Least Squares.

As soon as a movement is recorded by the spot sensors, the direction of movement is identified by the phase of the signal. Depending on the direction of movement, the time

taken by the object to move from the FoV of one spot sensor to another is calculated. Let the time taken be  $t$  s. Assuming that the object is moving in the center of FoV ( $R/2$ ), parallel to the tower face, we can calculate the speed of the object Speed =  $d_{FoV}/t$ , where  $d_{FoV}$  is the distance between the outer edge of one of the spot sensor and inner edge of another spot sensor at the center of FoV ( $d_{FoV}$  is constant as we know the angle of FoV). The speed thus obtained is first approximate speed of movement  $S_f$ .

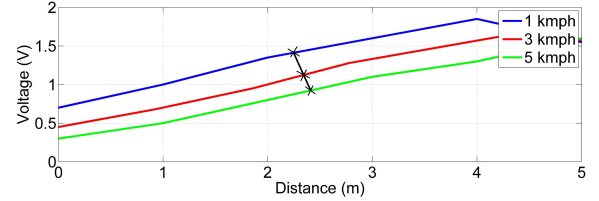


Figure 15: Example of interpolation of data for M3, from 1 kmph and 5 kmph curves to obtain  $S_f = 3$  kmph.

Since we have empirical curves for various speeds, we try to use the values from the curves directly. However, for a particular speed, if we do not have an empirical curve, we compute its value as described here. To find an intermediate curve set for speed  $S_f$ , we interpolate the available two set of curves whose speeds are above and below  $S_f$ . For instance, if  $S_f = 3$  kmph, then its curve set can be obtained by interpolation of curves of 1 kmph and 5 kmph. Figure 15 shows the interpolation of two curves for sensor M3 to obtain  $S_f = 3$  kmph.

For approximate distance calculation with the reference or interpolated curves, we need to find the least error between peak-to-peak amplitude of the signal generated by all multi-lens sensors. Let  $A_x^p$  represent the peak-to-peak amplitude from sensor  $x$ . We utilize the Least Squares method to find the least error,  $\epsilon_{x,S}(d)$ , for sensor  $x$  with reference speed  $S$  by using the following expression,

$$\epsilon_{x,S}(d) = \min(A_x^p - A_{x,S}(d))^2$$

The expression is iterated over different distances in the curve from  $d=1$  m to  $2d_{max}$  (the detection range) with  $S = S_f$ . The first approximation for range  $d_f$  is found when the error is minimized.

The distance  $d_f$  thus obtained is considered for refining the speed by replacing  $d_{FoV}$  with  $d_f$ . Thus, the newly found approximate speed is  $d_f/t$ . A new curve set for this speed has to be interpolated from the reference set of curves using Least Squares in each iteration. The process is iterated until the distance starts diverging instead of converging or if the pre-determined maximum number of iterations is reached. The algorithm for distance and speed calculation is shown in Algorithm 1. We set  $K = 10$ ; we observed that well within  $K$ , the algorithm converged and on few occasions it indeed diverged. A situation might occur where the moving object crosses the FoV of only one spot sensor returns without crossing the other. In this case, the pulse width of the signal gives the time required to calculate the first approximated speed.

## 7. EVALUATION

We evaluated the system and its behavior for different movement scenarios. It was also necessary to evaluate how

---

**Algorithm 1** Range estimation algorithm

---

```

1: procedure RANGEESTIMATION( $K$ ) //  $K$  is the maximum number of iterations for computing the range
2:    $d_{FoV} \leftarrow 4$  //in m
3:    $t \leftarrow$  time between two pulses
4:    $S \leftarrow d_{FoV}/t$ 
5:    $R_1 \leftarrow$  Find range using curves (as in Sec. 6.2.3)
6:    $i \leftarrow 1$ 
7:   repeat
8:      $S_i \leftarrow R_i/t$ 
9:      $R_{i+1} \leftarrow$  Find range using curves with  $S_i$ 
10:    if  $R_{i+1}-R_i < threshold$  then
11:      return  $R_i$ 
12:     $i \leftarrow i + 1$ 
13:   until  $i == K$ 
14:   return  $R_{i+1}$ 

```

---

well the sensor tower can locate an object even in the presence of obstacles. Hence, the experiment was conducted in a classroom as it contained many desks and benches as obstacles. We explain the scenarios and our evaluation in this section.

## 7.1 Deployment Scenarios

Distance and speed of movement of an object can be estimated using a single sensor tower but localizing the object is tricky since it can be located on any point at that particular distance. In order to locate the object in the FoV in two dimensions, we used two sensor towers that were spatially separated as shown in Figure 16. The towers were placed at  $90^\circ$  angle with respect to each other. One tower gave the abscissa and another provided the ordinate in the detection area. The towers were placed at a distance of  $d_{max}$  from a point which formed the center point of detection range of both the towers. These two towers were connected to a signal processing unit (laptop running MATLAB). Since the usage of three towers at an angle of  $120^\circ$  to each other did not add much information for trilateration, we used only two sensor towers to locate an object in two dimensions.

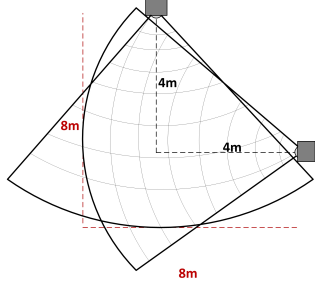


Figure 16: Sensor tower deployment.

In order to classify, the amplifier gain for all the sensors has to be the same and they should cover the required range. On the contrary, different zones are created by setting variable gains for different sensors for localization. So, it was not possible to classify and localize the object with the same sensor tower simultaneously. Hence, we used two sensors placed side-by-side, one for classification and the other for locating the abscissa of the object in the area of interest. However, if a digital potentiometer (software controller) were to be used

for controlling the amplifier gains, then it would be possible to classify and localize using the same sensor tower, though one after the other. In this case, all the sensors will have equal amplifier gain for ranging larger distance in the beginning. As soon as an object is detected within the range, we can classify the object. Immediately after classification, zones can be created by changing the gains via digital potentiometer for localization. In this manner, a single sensor tower could switch between classification and localization when a software controlled potentiometer is used for gain adjustments.

### 7.1.1 Zone creation

Since we wanted to have a higher resolution of localization, we chose an inter-zonal distance of 1 m. Therefore, the gains for sensors M1, M2, M3 and M4 were set so that they generate maximum peak-to-peak amplitude at 2 m, 3 m, 4 m and 1 m respectively at speed  $S_{min}$ . Since M3 covered the largest range of 4 m, both the towers were placed at 4 m distance from the center point (4 m, 4 m) in the area of interest. The maximum distance until which localization could be achieved was at  $2d_{max} = 8$  m from each tower as M3 can sense until  $2d_{max}$ .

### 7.1.2 Creating Reference curves

Three reference speeds  $S_{min}$ ,  $S_i$  and  $S_{max}$  were chosen to be 1 kmph, 5 kmph and 10 kmph respectively. This is because the speed ranges between 1 kmph, 5 kmph and 10 kmph are likely to be the speeds at which people move in indoors. With these values, the reference set of curves were created by moving in front of the tower (parallel to the face of a tower) at different distances ranging from 1 m to 8 m. The reference curves thus obtained are shown in Figure 14. Though we show only three sets of reference curves in the figure we have experimented for multiple sets of curves to evaluate the algorithm.

### 7.1.3 Movement scenarios

Typically, placing of the sensors is such that objects mostly do not move perpendicular to their FoV. Such scenarios were also tested and validated. The scenarios are as follows:

*Moving parallel to a tower and perpendicular to the other:* In this type of movement, the multi-lens sensors, from the tower to which the object is moving parallel, generate a sinusoidal swing with non-varying peak-to-peak amplitude over time. The multi-lens sensors of the tower, to which the movement direction is perpendicular, generate sinusoidal swings with varying amplitude over time. The amplitude increases when the movement is towards the tower and decreases when the object moves away from the tower. The object moving in the area to the left of the FoV of sensors and moving perpendicular to the tower can be identified since detection is triggered only by the left spot sensor.

*Moving at an angle to both the towers:* When the object moves at an angle to both the sensor towers, an increase or decrease in amplitude and frequency is observed. We find and use the angle as described in Section 4.

### 7.1.4 Testing and Validation

All the three sensor towers were connected to a PC on which the signal processing was done. However, the use of PCs can be eliminated by converting the MATLAB code into microcontroller compatible code to accomplish signal pro-

cessing on the microcontroller. The testing was performed for different speeds between  $S_{min}$  and  $S_{max}$  by moving in the area of interest at different distances and orientations. The trials were done with 20 different people. This included all the possible movement scenarios in the indoor location.

### 7.1.5 Comparison with Zappi et al.

We arranged our sensor towers to replicate the work by Zappi et al. [16]. We used only one sensor from each tower and masked the multi-lens to mimic their setup. We used three single sensor mounts as shown in Figure 17 of our setup to compare with their work for reference. They find *only* the direction of movement (only left-to-right or otherwise) using spatial diversity induced by their deployment. We use collocated sensors in a single tower. Indeed we improved their work by applying the techniques described in the earlier sections to find the distance in their deployment for comparison. We use the geometry of the deployment and the signals captured by three sensors to find the range. If the object moves at an angle, it is difficult to estimate the distance with their setup. Though there are many differences such as above, it is the closest work to ours.



Figure 17: Setup for comparing our work with [16].

## 7.2 Results and Discussions

The different classification levels - very short, short, tall and very tall heights are imitated (by walking, crawling, etc.) multiple times by 20 different people. The confusion matrix thus obtained for different trials is listed in Table 3. We observe that the values along the diagonal show higher than 90% accuracy. We evaluated the error probability

Table 3: Confusion matrix obtained for different classification types.

|            | Very short | Short | Tall | Very tall |
|------------|------------|-------|------|-----------|
| Very short | 0.98       | 0.02  | 0    | 0         |
| Short      | 0.06       | 0.9   | 0.04 | 0         |
| Tall       | 0          | 0     | 0.93 | 0.07      |
| Very tall  | 0          | 0     | 0.05 | 0.95      |

distribution for localization at longer distances by increasing the range of M1 to 11m and M3 to 9m. Figure 18 shows the error probability distribution of localization over all distances till 10m moving at different angles. At shorter distances, as seen in Figure 6 the amplitude is less resulting in higher errors. Further, at shorter distances noise also affects the range calculations. Around 5m range since all the sensors capture the movement well, the amplitude is relatively higher resulting in better positioning. Beyond this distance, since only one or two sensors capture the movement the range calculations are affected.

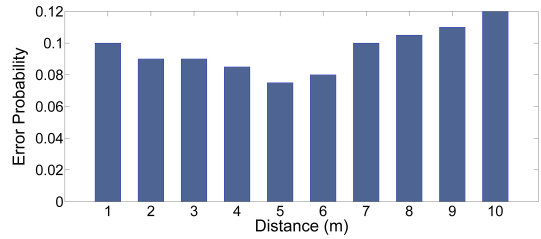


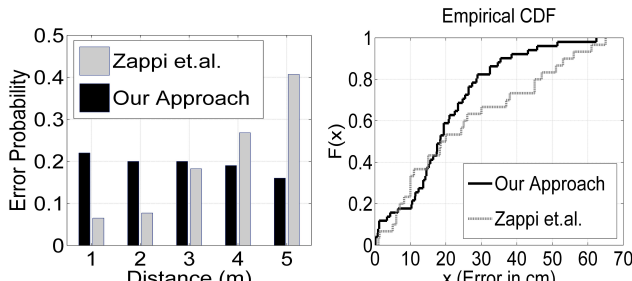
Figure 18: Error probability distribution over distances for localization.

The probability distribution of error for localization in three major scenarios at different speeds are listed in Table 4. In the table, we observe that for all the speeds, the error probability is relatively more for the movement perpendicular to the tower face as compared to parallel and at different orientations. This is because, when a person moves towards the tower in between S1 and S3 along the center, the person is usually in the FoV of one lenslet of a multi-lens sensor (hardly two or three). As the detection is hardly triggered in adjacent lenslets of the center lenslet, a sinusoidal swing is not generated by multi-lens sensors. Even when the person approaches the tower, most of the lenslets are triggered at the same time, generating multiple high peaks without generating sinusoidal wave. However, the column ‘perpendicular to tower’ in Table 4 includes all movement scenarios such as moving perpendicular to S1, perpendicular to the tower in between S1 and S3 and perpendicular to S3. The major contribution towards the error is perpendicular movement in the center of FoV, in between S1 and S3. The results are more accurate for movements parallel to the tower. For angled movements, the error is relatively high at lower speeds as the dampening of sinusoidal swing cannot be observed clearly at very low amplitudes.

Table 4: Error probability distribution for localization in different scenarios at different speeds and distances.

| Speed (kmph) | Error probability      |                   |            |
|--------------|------------------------|-------------------|------------|
|              | Perpendicular to tower | Parallel to tower | At angles. |
| 1            | 0.42                   | 0.2               | 0.38       |
| 2            | 0.51                   | 0.17              | 0.32       |
| 3            | 0.49                   | 0.18              | 0.33       |
| 4            | 0.56                   | 0.16              | 0.28       |
| 5            | 0.61                   | 0.14              | 0.25       |
| 6            | 0.64                   | 0.12              | 0.24       |
| 7            | 0.63                   | 0.15              | 0.22       |
| 8            | 0.55                   | 0.19              | 0.26       |
| 9            | 0.52                   | 0.20              | 0.28       |
| 10           | 0.48                   | 0.21              | 0.31       |

We compare our work with Zappi’s set up. Note that in our method for ranging we used single tower. Figure 19a shows an interesting aspect that while error probability in our case remains constant, Zappi’s method shows an increase. This is due to the fact that at lower ranges the signal amplitude is higher and it goes down with distance. In our case, we control the gain for ranging. We also plot CDF in Figure 19b comparing our method with Zappi’s set up for localization within 5m. It is evident that 50% of the times both the methods behave almost similarly having an error around 20 cm and 80% of the times we achieve within 30 cm accuracy. Where as in Zappi’s case it is around 50 cm.



(a) Error probability over distances. (b) CDF of error and distance in localization.

Figure 19: Comparison of proposed method with [16].

While localizing objects up to 10 m (not shown) we found that 50% of the times the error is below 60 cm.

## 8. CONCLUSIONS

Typically, PIR sensors are used to provide a binary output to detect moving objects in its FoV. This limits the collected information about the targets. Thus we tapped the analog signals from the sensors that made it possible to easily capture angle and direction of movement, speed, etc. To effectively capture the analog signals we used a tower with a pair of spot sensors and a pair of multi-lens sensors. Using the tower we provided a thorough characterization of analog signals. We also changed the gain of each sensor so as to cover different ranges. Further, we found empirically an expression between the range and peak-peak amplitude for multi-lens sensors. This provides us a handle to explore localization possibilities. We have also provided a methodology to derive sets of reference curves that capture the relation among amplitude, distance and speed in various scenarios. Using these, we experimented with localization employing two sensor towers. The results are significant: we could achieve improved detection reducing the false positives. Further, using a single tower we found 50% of the times localization is within an error bound of 60 cm when the range is up to 10 m. The error also depends on the range of the sensors. Moreover the cost of electronic circuitry for the tower is around \$15. The power requirement for each sensor is approximately 1.67 mW including amplifier circuitry. Thus, we can achieve a reasonably high accuracy in localization with low power and inexpensive PIR sensors.

There are some limitations though: we still need to find a way to switch online PIR sensors from detection mode to ranging mode. Since the operating voltages are too small, the possibility of localization error is higher. The time for localization is around 4 s since it depends on the speed of the object and time taken to move across the FoV. This estimation time is on the higher side. We have tested our system with only one person in the FoV. However, if there is more than one person our system may not work. We are in the process of addressing these limitations.

## Acknowledgement

Authors would like to thank National Science Foundation (NSF) and Department of Electronics and Information Technology (DeitY) under the Indo-US Pervasive Communications and Computing Collaboration (PC3) initiative.

## 9. REFERENCES

- [1] Melexis mlx90620 firray:16x4 far infrared array. <http://www.melexis.com/Infrared-Thermometer-Sensors/Infrared-Thermometer-Sensors/MLX90620-776.aspx>. Accessed: 2015-02-20.
- [2] Panasonic grid-eye infrared array sensor. <http://na.industrial.panasonic.com/products/sensors/sensors-automotive-industrial-applications/grid-eye-infrared-array-sensor>. Accessed: 2015-02-20.
- [3] Microsoft kinect. <http://www.xbox.com/en-US/xbox-one/accessories/kinect-for-xbox-one>, 2014. [Online; accessed 20 Oct. 2014].
- [4] R. Abu Sajana, R. Subramanian, P. Kumar, S. Krishnan, B. Amruth, J. Sebastian, M. Hegde, and S. Anand. A low-complexity algorithm for intrusion detection in a pir-based wireless sensor network. In *5th International Conference on Intelligent Sensors, Sensor Networks and Information Processing (ISSNIP)*, pages 337–342, Dec 2009.
- [5] L. Adrian and L. Ribickis. Design of human tracking robot utilizing pyroelectric sensor and analogue circuitry. In *IEEE EUROCON*, pages 1927–1931, July 2013.
- [6] I. Al-Naimi, C. B. Wong, P. Moore, and X. Chen. Advanced approach for indoor identification and tracking using smart floor and pyroelectric infrared sensors. In *5th International Conference on Information and Communication Systems (ICICS)*, pages 1–6, April 2014.
- [7] G. Feng, Y. Yang, X. Guo, and G. Wang. A compressed infrared motion sensing system for human-following robots. In *11th IEEE International Conference on Control Automation (ICCA)*, pages 649–654, June 2014.
- [8] A. Frankiewicz and R. Cupek. Smart passive infrared sensor - hardware platform. In *39th Annual Conference of the IEEE on Industrial Electronics Society, IECON*, pages 7543–7547, Nov 2013.
- [9] S. Lee, K. N. Ha, and K. C. Lee. A pyroelectric infrared sensor-based indoor location-aware system for the smart home. *IEEE Transactions on Consumer Electronics*, 52(4):1311–1317, Nov 2006.
- [10] X. Lv and Y. Liu. Design of human motion detection and tracking robot based on pyroelectric infrared sensor. In *8th World Congress on Intelligent Control and Automation (WCICA)*, pages 3737–3740, July 2010.
- [11] A. Moragrega and C. Ibárs. Performance analysis of cooperative and range based localization algorithms for zigbee and 802.15.4a wireless sensor networks. In *IEEE 21st International Symposium on Personal Indoor and Mobile Radio Communications (PIMRC)*, pages 1996–2001, Sept 2010.
- [12] R. Upadrashta et al. An animation-and-chirplet based approach to intruder classification using pir sensing. In *Proc. 10th International Conference on Intelligent Sensors, Sensor Networks and Information Processing (ISSNIP) (DISC 2015)*. IEEE, 2015.
- [13] F. Wahl, M. Milenkovic, and O. Amft. A distributed pir-based approach for estimating people count in office environments. In *IEEE 15th International Conference on Computational Science and Engineering, CSE '12*, pages 640–647, Washington, DC, USA, 2012. IEEE Computer Society.
- [14] Y. Wang, Q. Jin, and J. Ma. Integration of range-based and range-free localization algorithms in wireless sensor networks for mobile clouds. In *IEEE Green Computing and Communications (GreenCom)*, pages 957–961, Aug 2013.
- [15] J. Yun and M.-H. Song. Detecting direction of movement using pyroelectric infrared sensors. *IEEE Sensors Journal*, 14(5):1482–1489, May 2014.
- [16] P. Zappi, E. Farella, and L. Benini. Enhancing the spatial resolution of presence detection in a pir based wireless surveillance network. In *IEEE Conference on Advanced Video and Signal Based Surveillance*, pages 295–300, Sept 2007.
- [17] P. Zappi, E. Farella, and L. Benini. Pyroelectric infrared sensors based distance estimation. In *IEEE Sensors*, pages 716–719, Oct 2008.
- [18] P. Zappi, E. Farella, and L. Benini. Tracking motion direction and distance with pyroelectric ir sensors. *IEEE Sensors Journal*, 10(9):1486–1494, Sept 2010.
- [19] Z. Zhang, X. Gao, J. Biswas, and J. K. Wu. Moving targets detection and localization in passive infrared sensor networks. In *10th International Conference on Information Fusion*, pages 1–6, July 2007.